Immobilization of ZnO nanoparticles on fluorinated perlite granules for the photocatalytic degradation of methylene blue

Nguyet Anh Pham, Thi Huynh Nhu Nguyen, Tuan Ngoc Tran, Quy Tu Nguyen, Tien Khoa Le*

University of Science - Vietnam National University, Ho Chi Minh City

Received 15 June 2017; accepted 11 September 2017

Abstract:

The fluorination of perlite granules and the immobilization of ZnO nanoparticles on the perlite surface were carried out at the same time by a simple impregnation method to create new highly photocatalytic materials which are easily separated from reaction solutions after treatment. The influence of perlite fluorination on the crystal structure, morphology, UV-visible absorption, and surface functional groups of ZnO, as well as on the ZnO content on perlite, was respectively characterized by XRD, FE-SEM, UV-Visible diffuse reflectance, FTIR and atomic absorption spectrometry. The photocatalytic activity was evaluated via the extent of degradation of methylene blue under UVA irradiation. According to the results, the fluorination of perlite leads to numerous effects on ZnO, such as the decline of ZnO cell parameters, the increase of ZnO content on perlite granules (resulting in the enhancement of light absorption in UVA range), and the decrease of ZnO particle size, which can effectively improve its photocatalytic performance. The photocatalysts were also found to be able to stay afloat on water, allowing for easy separation from the reaction solution.

Keywords: ***coating, fluorination, perlite granules, photocatalytic activity, ZnO nanoparticles.***

Classification number: ***2.2***

Introduction

Due to their chemical structure and stability, most of the dyestuffs used in the textile industry, including methylene blue, are resistant to solvents and are difficult to eliminate by conventional wastewater treatment methods such as cost-effective biological techniques [1-3]. Although it is not a strongly toxic compound, exposure to methylene blue can cause rapid pulse, shock, cyanosis, and tissue necrosis in humans [4]. Hence, the release of waste water containing methylene blue can lead to harmful environmental effects and damages to human health. Over the past few decades, the use of semiconductor photocatalysts based on TiO_2 nanopowders has proven to be a promising method of waste water treatment since various organic pollutants including methylene blue and other organic dye molecules can be completely degraded under UV irradiation in the presence of these photocatalysts [5-9]. Besides TiO_2, ZnO is another semiconductor which has been investigated in recent years as an excellent material for photocatalytic processes owing to its photosensitivity, high stability, and low toxicity [10, 11]. In some photodegradation experiments, ZnO nanopowders exhibit activity superior to that of TiO_2 for the treatment of dye wastewater [12, 13]. However, there are two major drawbacks for the application of these suspended particles in practical wastewater treatment procedures: (i) the scattering of UV light by nanoparticles can limit photocatalytic activity and (ii) the catalytic nanoparticles are difficult to separate from the reaction solution [14]. Therefore, it is necessary to immobilize semiconductor photocatalysts on solid substrates in order to solve these problems.

Many materials have been studied for the immobilization of photocatalytic TiO_2 particles, such as glass [14, 15], stainless steel plate [16, 17], polymers [18, 19], alumina [20], and ceramics [21]. Recently, Hosseini, et al. [22] investigated the immobilization of TiO_2 on perlite granules for the photocatalytic degradation of phenol. Granular perlite is an amorphous volcanic glass with high porosity, making it suitable as a potential substrate for TiO_2 nanopowder. The second advantage of perlite granules is that they are very light, which allows

*Corresponding author: Email: ltkhoa@hcmus.edu.vn

them to stay afloat on the surface of wastewater [22]. As a result, the TiO_2 photocatalyst coated on perlite granules is easily exposed to the available radiation source to ensure efficient light absorption [22, 23]. Unfortunately, the coating of TiO_2 particles is mostly distributed on the external surfaces of perlite granules [23] which usually consist of smooth flat layers. This may limit the mechanical adhesion between photocatalytic particles and the perlite surface and then hinder the immobilization of nanopowders. Thus the surface of perlite granules still needs to be modified in order to make it an effective substrate for photocatalysts.

However, so far, up to our best knowledge, no research has been conducted on the modification of perlite surfaces for the immobilization of ZnO catalysts. Since perlite granules are mainly composed of SiO_2 (73%) [24], it is suggested that fluoride ions can modify the perlite surface by slowly corroding its silica components. Therefore, in this work, we have prepared new photocatalytic materials based on ZnO nanoparticles coated on fluoride-modified perlite granules by a simple one-step impregnation method in order to improve the bonding between ZnO particles and perlite substrate and then enhance their photocatalytic activity. The influence of fluoride contents used to modify perlite surfaces on the coating of ZnO and the photocatalytic performance were also investigated.

Experimental section

Sample preparation

The starting materials $Zn(NO_3)_2.6H_2O$, $K_2C_2O_4.H_2O$ and KF (99%, extra pure grade) were purchased from Sigma Aldrich. Methylene blue (MB) (analytical grade) was purchased from Merck. These chemicals were used as received without further purification. Perlite granules obtained from Ninh Binh province (Vietnam) were treated with H_2SO_4 solution (2 mol/l) at 80 - 100°C for 30 minutes. Distilled water was used in all the experiments.

For the preparation of ZnO coated on fluoride-modified perlite granules, firstly, $Zn(NO_3)_2.6H_2O$ was separately dissolved in water to obtain 250 ml of Zn^{2+} solution (1 mol/l). Then 5 g of perlite granules were added to this Zn^{2+} solution under regular stirring at room temperature. After that, 250 ml of a solution containing both $K_2C_2O_4$ (1 mol/l) and KF (the KF concentration varied from 1 to 3 mol/l) was added to the Zn^{2+} solution to fluorinate the surface of the perlite granules and to create the white ZnC_2O_4 precipitate deposited on their surface. The slurry containing perlite granules was regularly stirred for 30 minutes for the fluorination. Next, these perlite granules were separated from the slurry, washed with distilled water, dried at 150°C for two hours, and heated in air at 500°C for two hours. In the following manuscript, these samples were labelled as PZnOF-X (X is equal to 1, 2, and 3 corresponding to the KF concentration of 1, 2, and 3 mol/l, respectively).

ZnO was also coated on bare perlite granules (labelled as PZnO) by the same process without using KF. Moreover, fluorinated perlite granules without ZnO immobilization were prepared by stirring 5 g of granular perlite in 500 ml of KF solution (1 mol/l) and then dried at 150°C during two hours in order to investigate the effects of fluorination on granular perlite.

Characterization

The surface morphology and particle size of PZnO and PZnOF-X catalysts were studied by field emission scanning electron microscopy (FE-SEM) using a HITACHI S-4800 with an acceleration voltage at 10 kV. FE-SEM micrographs of bare perlite granules and fluorinated perlite granules without ZnO immobilization were also taken. Their specific surface area was measured with a NOVA 1000e instrument and calculated using the BET (Brunauer-Emmett-Teller) equation.

The crystalline structure and phase composition of PZnO and PZnOF-X samples were characterized by powder X-ray diffraction (XRD) measurements, which were carried out by a BRUKER-Binary V3 X-ray diffractometer using Cu Kα radiation (λ = 1.5406 Å). The accelerating voltage and the applied current were 40 kV and 40 mA, respectively. The Rietveld refinements were carried out using Fullprof 2009 structure refinement software [25].

In order to investigate the surface functional groups of prepared catalysts, their FT-IR spectra were recorded in the 4000-400 cm^{-1} frequency range at room temperature using a Bruker VERTEX 70 spectrometer.

The quantity of ZnO coated on the surface of different perlite samples was evaluated by atomic absorption spectrometry using a Shimadzu AA-6300 spectrometer. The ZnO/perlite and FZnO/perlite samples were separately ground into fine powder with a mortar and pestle and then stirred in HCl solution (6 mol/l) for 24 hours. Then the quantity of Zn^{2+} ions was measured at a wavelength of 213.9 nm.

UV-Visible diffuse reflectance spectra of the catalysts were measured using a Perkin-Elmer Lamda 850 Spectrophotometer which is equipped with a 15 cm diameter integrating sphere bearing the holder in the bottom horizontal position and calibrated with a certified Spectralon white standard (Labsphere, North Sutton, USA). The spectra were recorded at room

temperature in steps of 1 nm, in the range of 300-400 nm with a bandwidth of 2 nm.

Photocatalytic tests

The photocatalytic activities of PZnO and PZnOF-X samples were evaluated via the degradation of MB. The photocatalytic reactor consists of a glass beaker containing 250 ml of MB solution (10^{-5} mol/l) with 2.0 grams of catalysts, cooled by continuous water flow and stirred continuously by a mechanic agitator. The outer wall of the reactor is covered with an aluminium layer to block out any exterior light. The pH of suspensions was fixed at 7 and the reaction temperature was maintained at 30°C during the experiments. Prior to the irradiation, the solution containing catalysts was stirred for 60 minutes in the dark in order to obtain the MB adsorption equilibrium. Then the reaction solution was irradiated by an 8-W UV Philips light lamp placed about 10 cm above the solution surface. During the illumination, 5 ml of suspension was sampled and analyzed with an SP-300 Optima spectrophotometer.

Results and discussions

Figures 1A and 1B present the FE-SEM micrographs of perlite granules before and after fluorination, respectively. It was observed that the surface of bare granular perlite is composed of relatively smooth terraces which are randomly oriented and superimposed on each other. When the perlite sample was fluorinated, the surface was clearly corroded with increased roughness and the appearance of various shallow holes. BET measurements also indicated the increase of the specific surface area of perlite granules from 0.415 to 0.498 m^2/g when fluorinated, confirming the corrosion role of KF on perlite which may improve the immobilization of ZnO nanoparticles on the perlite surface. For

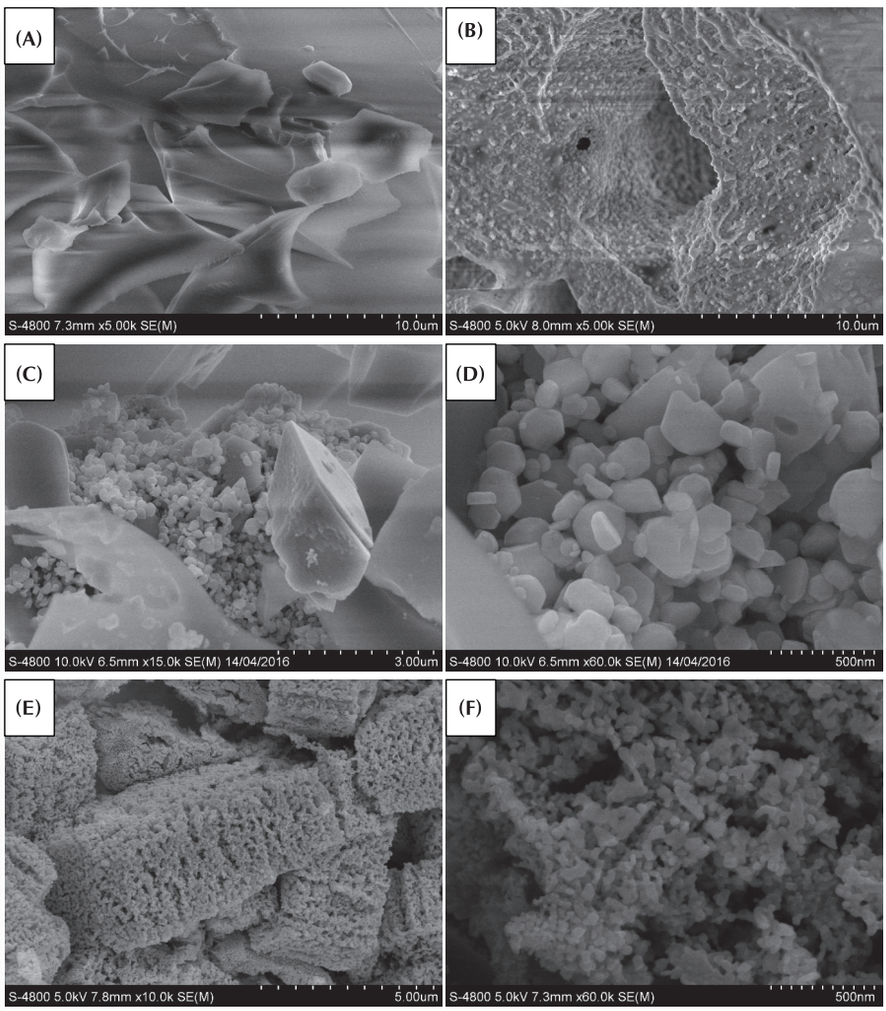

Fig. 1. FE-SEM micrographs at different magnifications of perlite granules (A), fluorinated perlite granules (B), PZnO (C, D) and PZnOF-2 (E, F).

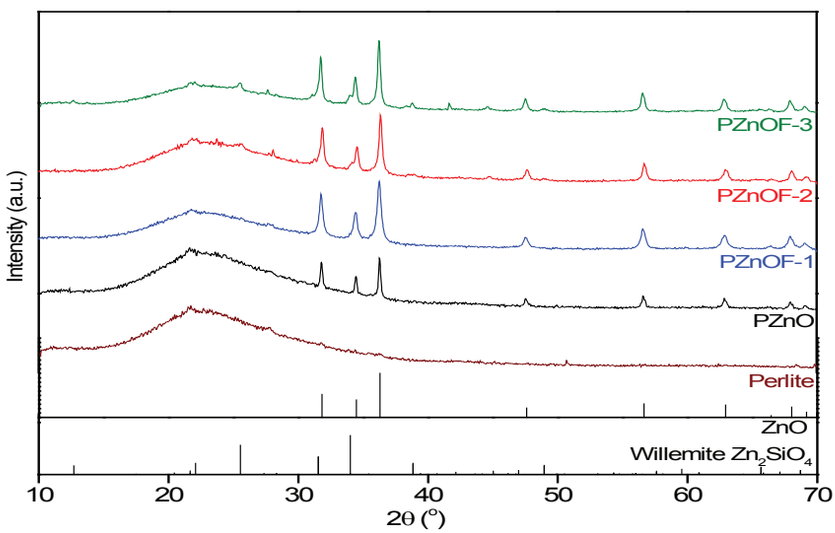

Fig. 2. XRD patterns of perlite, PZnO and fluorinated PZnO samples.

the PZnO sample, Fig. 1C and Fig. 1D display the presence of ZnO polyhedral particles, which demonstrates the successful immobilization of ZnO on the surface of perlite. These particles were found to be non-uniform in size (with a diameter of 100 - 300 nm) and tended to agglomerate. When ZnO was coated on fluorinated perlite (Fig. 1E and Fig. 1F for PZnOF-2 sample), the ZnO particles also appeared in large agglomerates but their particle size was reduced to around 50 nm. It should be noted that in this sample, nearly all the surfaces of fluorinated perlite granules were covered with ZnO nanoparticles whereas in the PZnO sample, the perlite surface was only partially covered with ZnO. Therefore, it seems that the fluorination of perlite does not only reduce the ZnO particle size but also increases the ZnO content on the perlite surfaces.

Powder XRD was used to follow the effects of perlite fluorination on the crystallite structures and phase compositions of ZnO coated on perlite granules. From Fig. 2, the perlite sample shows the XRD pattern in an arc-shaped baseline without any diffraction peak, confirming the amorphous structure of these granules, which is in agreement with Hosseini's findings [22]. For the pattern of PZnO powder, we observed a series of characteristic peaks at 31.77° ((100) line), 34.43° ((002) line), 36.26° ((101) line), 47.55° ((102) line) and 56.60° ((110) line). These diffraction peaks are in accordance with the zincite phase of ZnO (space group P63mc, JCPDS No. 36-1451), which confirms that ZnO was successfully deposited on the surface of perlite granules. Moreover, when coating ZnO on fluorinated perlite with increasing KF concentration from 1 to 2 mol/l, no peaks of impurity were observed, suggesting that the fluorination did not modify the phase composition of ZnO. However, for the PZnOF-3 sample, the XRD pattern showed the apparition of willemite Zn_2SiO_4 phase (space group R-3, JCPDS No. 37-1485), identified by the diffraction peaks at 21.68°, 25.31° and 41.60°. The formation of this additional crystallographic phase may be attributed to the reaction between ZnO and the silicate components in the perlite composition, which was promoted by the addition of KF. Furthermore, it was observed that the cell parameters of ZnO were modified by the fluorination (Table 1). When ZnO was immobilized on fluorinated perlite with increased fluoride content, the cell parameters and the cell volume were decreased.

Table 2 represents the ZnO content in our samples measured by calculating the Zn concentration via atomic absorption spectrometry. The PZnO sample only contains 8.08 mg Zn g^{-1} product. For ZnO nanoparticles immobilized on fluorinated perlite, the ZnO content was strongly increased, which is consistent with the observation in the FE-SEM study. The highest ZnO content was found in the PZnOF-2 sample with 71.44 mg Zn g^{-1} product - nearly 9 times higher than that found in the PZnO sample. This result suggests that KF may corrode the silicate component of perlite surfaces during the fluorination to improve the coating of ZnO. However, when KF concentration was increased to 3 mol/l, the ZnO content dramatically decreased (28.45 mg Zn g^{-1} product), indicating that a high KF amount is capable of damaging the surface of perlite granules and thus lowering the bonding between ZnO nanoparticles and perlite granules.

Figure 3 presents the FT-IR spectra of PZnO and PZnOF-2 samples. From these spectra, two broad absorption peaks were observed around 1053.06 and 789.04 cm^{-1}, which are attributed to the stretching vibrations of Si-O and Si-O-Si bonds on the surface of perlite granules [26]. These spectra also display a sharp peak at 459.74 cm^{-1} due to the stretching vibration of Zn-O [27], confirming the presence of ZnO deposited on the perlite surface. For the PZnO sample, another weak peak was detected at 1384.13 cm^{-1}. This peak may be ascribed to the C-O vibration originated from the adsorption of CO_2 on the surface of perlite granules [28, 29]. Nevertheless, this peak disappeared when the ZnO-perlite system was fluorinated. It should be noted that the fluorination of perlite promotes the coating of ZnO onto perlite granules, which may cover all the perlite surface and then hinder its adsorption of CO_2.

The optical responses of PZnO and PZnOF-2 samples were analyzed using UV-visible diffuse reflectance spectroscopy (Fig. 4). The spectrum of PZnO material shows a broad absorption band in the UV range below 400 nm (maximum absorption at the wavelength of 200-300 nm). When ZnO was immobilized on fluorinated perlite, the intensity of the absorption band in the visible zone slightly decreased whereas the absorption peak of the UV region

Table 1. Cell parameters and cell volumes of ZnO in PZnO and PZnOF samples.

Sample	Cell parameters		Cell volume (Å^3)
	a (Å)	*c (Å)*	
PZnO	3.25097	5.20838	47.67154
PZnOF-1	3.25031	5.20688	47.63846
PZnOF-2	3.24954	5.20495	47.59824
PZnOF-3	3.2493	5.20428	47.58509

Table 2. ZnO content and rate constant of MB bleaching under UVA light illumination on PZnO and PZnOF samples.

Sample	ZnO content determined by AAS (mg Zn g^{-1} sample)	Rate constant of MB bleaching under UVA illumination (h^{-1})
PZnO	8.08	0.33
PZnOF-1	21.31	0.87
PZnOF-2	71.44	1.23
PZnOF-3	28.44	0.90

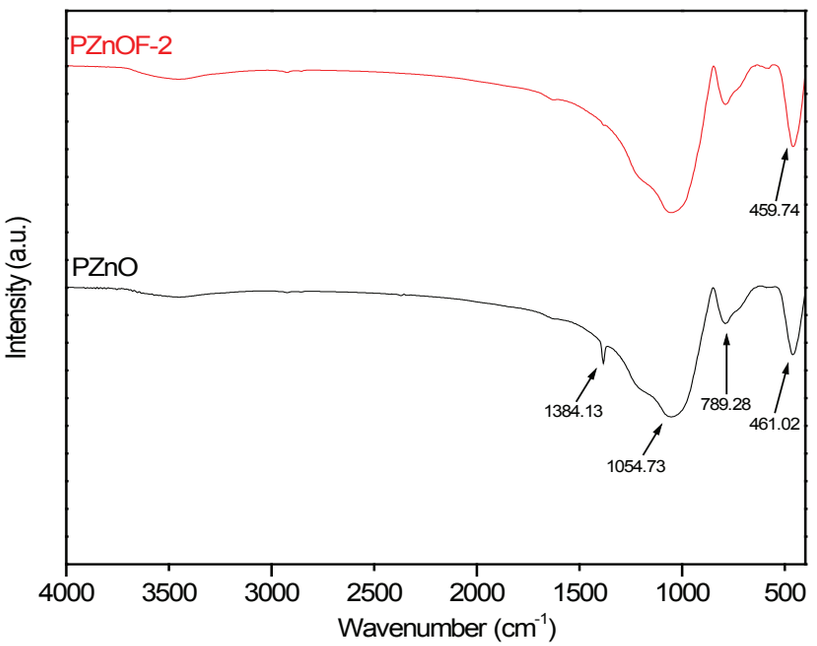

Fig. 3. FTIR spectra of PZnO and PZnOF-2 samples.

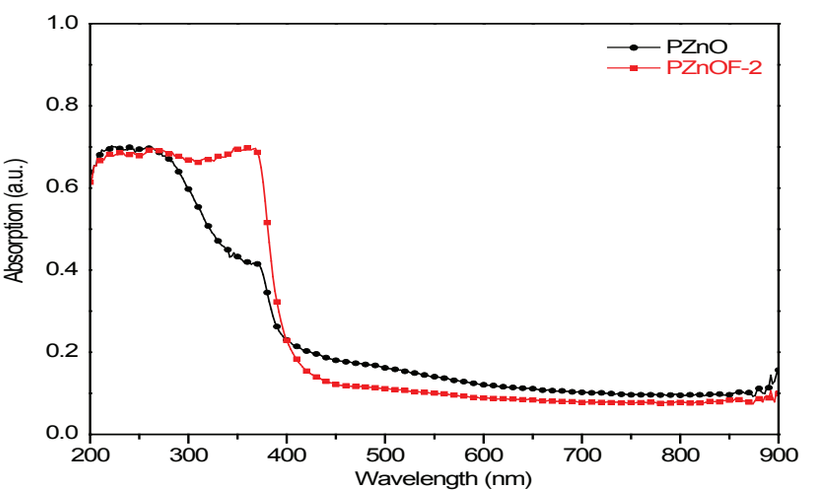

Fig. 4. UV-visible absorption spectra of PZnO and PZnOF-2 samples.

strongly rose in the range of 300-400 nm. This enhanced UV absorption of the PZnOF-2 sample can also be explained by the increase of ZnO content owing to the fluorination of perlite.

The UVA light induced photocatalytic activity of PZnO and PZnOF samples was evaluated via the photocatalytic MB degradation. The time-dependent profiles of MB degradation in the presence of our catalysts under UVA light irradiation (Fig. 5) prove that the net decomposition of MB in the aqueous solution followed the pseudo-first-order Langmuir-Hinshelwood kinetic model. Hence, the rate constant of this reaction was determined by plotting $\ln(C/C_0)$ versus time (C is the MB concentration at time t and C_0 is the initial MB concentration) and presented in Table 2. The catalytic tests indicated that the fluorination of perlite effectively improved the photocatalytic performance of ZnO supported on the perlite granules. In fact, the rate constant (k) of MB degradation in the presence of the PZnO sample only reached 0.33 h^{-1} whereas the PZnOF-2 catalyst showed the best performance with k = 1.23 h^{-1}, which was about four times higher than that of the PZnO catalyst. The increase of photocatalytic activity in our samples can be explained by two factors. Firstly, based on the atomic absorption spectra and UV-visible reflectance diffuse spectra, the fluorination of perlite was found to successfully modify the surface of perlite granules, which increased the ZnO content on the perlite surface and then enhanced the UVA absorption of catalysts. It has been reported that the high photon absorption can promote the formation of photogenerated electrons and holes and then improve the photocatalytic activity [7, 30]. Secondly, the fluorination of perlite also decreased the particle size of ZnO. As a result, the active sites of photocatalytic ZnO were enhanced by the perlite fluorination,

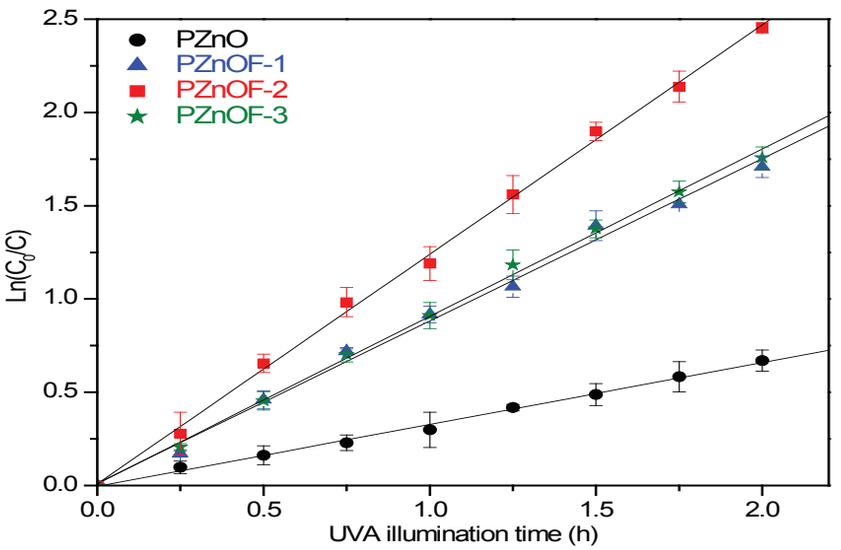

Fig. 5. Ln(C_0/C) versus time plot of MB bleaching under UV irradiation on PZnO and PZnOF samples. C is the MB concentration (mol/l) at time t and C_0 is the initial MB concentration (mol/l).

leading to the rise of photocatalytic properties. However, when the perlite surface was fluorinated more strongly, with a KF concentration of 3 mol/l, the ZnO content was decreased on the PZnOF-3 sample, resulting in a decline in photocatalytic performance.

These results showed that the immobilization of ZnO nanoparticles supported on fluorinated perlite granules may be a simple and efficient method to obtain highly photocatalytic materials which are easily separated from solutions after treatment.

Conclusions

In this study, ZnO nanoparticles were developed on fluorinated perlite granules with various KF concentrations by a simple one-step impregnation method in order to study the effects of perlite fluorination on the crystal structure, morphology, optical properties, ZnO content, and photocatalytic activity of ZnO/perlite. The experimental results showed that the fluorination of perlite does not only enhance the ZnO content on perlite surfaces, increasing the UVA absorption, but also decreases the particle size of ZnO. These modifications strongly improved the photocatalytic performance of our materials. The fluorinated sample prepared with KF concentration of 2 mol/l was found to be the optimal photocatalyst. When the KF concentration was further increased, the ZnO content on perlite granules dramatically decreased, leading to the reduction of photocatalytic activity.

ACKNOWLEDGEMENTS

The authors would like to thank the University of Science - Vietnam National University, Ho Chi Minh City for their technical support.

REFERENCES

[1] R. Asahi, T. Morikawa, T. Ohwaki, K. Aoki, Y. Taga (2001), "Visible-light photocatalysis in nitrogen-doped titanium oxides", *Science*, **293**, pp.269-271.

[2] E. Khelifi, H. Gannoun, Y. Touhami, H. Bouallagui, M. Hamdi (2008), "Aerobic decolourization of the indigo dye-containing textile wastewater using continuous combined bioreactors", *J. Hazard. Mater.*, **152**, pp.683-689.

[3] R.S. Dave, A.R. Patel (2010), "Photochemical and photocatalytic of cypermethrin under UV radiation", *Der pharma chemica*, **2**, pp.152-158.

[4] H. Ma, Q. Zhuo, B. Wang (2009), "Electro-catalytic degradation of methylene blue wastewater assisted by Fe_2O_3-modified kaolin", *Chem. Eng. J.*, **155**, pp.248-253.

[5] Y. Zhang, T. Oyama, A. Aoshima, H. Hidaka, J.C. Zhao, N. Serpone (2001), "Photooxidative N-demethylation of methylene blue in aqueous TiO_2 dispersions under UV irradiation", *J. Photochem. Photobiol. A*, **140**, pp.163-172.

[6] H. Lachheb, E. Puzenat, A. Houas, M. Ksibi, E. Elaloui, C. Guillard, J.M. Herrmann (2002), "Photocatalytic degradation of various types of dyes (Alizarin S, Crocein Orange G, Methyl Red, Congo Red, Methylene Blue) in water by UV-irradiated titania", *Appl. Catal. B*, **39**, pp.75-90.

[7] A. Vijayabalan, K. Selvam, R. Velmurugan, M. Swaminathan (2009), "Photocatalytic activity of surface fluorinated TiO_2-P25 in the degradation of Reactive Orange 4", *J. Hazard. Mater.*, **172**, pp.914-921.

[8] H. Shin, T.H. Byun, S. Lee, S.T. Bae, H.S. Jung (2013), "Surface hydroxylation of TiO_2 yields notable visible-light photocatalytic activity to decompose rhodamine B in aqueous solution", *J. Phys. Chem. Solids*, **74**, pp.1136-1142.

[9] T.K. Le, D. Flahaut, H. Martinez, H.K.H. Nguyen, T.K.X. Huynh (2015), "Study of the effects of surface modification by thermal shock method on photocatalytic activity of TiO_2 P25", *Appl. Catal. B*, **165**, pp.260-268.

[10] A. Segura, J.A. Sans, F.J. Manjon, A. Munoz, M.J. Herrera-Cabrera (2003), "Optical properties and electronic structure of rock-salt ZnO under pressure", *Appl. Phys. Lett.*, **83**, pp. 278-280.

[11] L. Jing, D. Wang, B. Wang, S. Li, B. Xin, H. Fu, J. Sun (2006), "Effects of noble metal modification on surface oxygen composition, charge separation and photocatalytic activity of ZnO nanoparticles", *J. Mol. Catal. A*, **244**, pp.193-199.

[12] K. Gouvea, F. Wypych, S.G. Moraes, N. Duran, N. Nagata, P. Peralta-Zamora (2000), "Semiconductor-assisted photocatalytic degradation of reactive dyes in aqueous solution", *Chemosphere*, **40**, pp.433-440.

[13] J. Han, Y. Liu, N. Singhal, L. Wang, W. Gao (2012), "Comparative photocatalytic degradation of estrone in water by ZnO and TiO_2 under artificial UVA and solar irradiation", *Chem. Eng. J.*, **213**, pp.150-162.

[14] M.A. Behnajady, N. Modirshahla, M. Mirzamohammady, B. Vahid, B. Behnajady (2008), "Increasing photoactivity of titanium

dioxide immobilized on glass plate with optimization of heat attachment method parameters", *J. Hazard. Mater.*, **160**, pp.508-513.

[15] S. Gelover, P. Mondragon, A. Jimenez (2004), "Titanium dioxide sol-gel deposited over glass and its application as a photocatalyst for water decontamination", *J. Photochem. Photobiol. A*, **165**, pp.241-246.

[16] J. Yu, H. Yu, C.H. Ao, S.C. Lee, J.C. Yu, W. Ho (2006), "Preparation, characterization and photocatalytic activity of in situ Fe-doped TiO_2 thin films", *Thin Solid Films*, **496**, pp.273-280.

[17] S.W. da Silva, J.B. Bortolozzi, E.D. Banús, A.M. Bernardes, M.A. Ulla (2016), "TiO_2 thick films supported on stainless steel foams and their photoactivity in the nonylphenol ethoxylate mineralization", *Chem. Eng. J.*, **283**, pp.1264-1272.

[18] Z. Niu, F. Gao, X. Jia, W. Zhang, W. Chen, K. Qian (2006), "Synthesis studies of sputtering TiO_2 films on poly(dimethylsiloxane) for surface modification", *Colloids Surfaces A: Physicochem. Eng. Aspects*, **272**, pp.170-175.

[19] J. Zeng, S.L. Liu, J. Cai, L. Zhang (2010), "TiO_2 immobilized in cellulose matrix for photocatalytic degradation of phenol under weak UV light irradiation", *J. Phys. Chem. C*, **114**, pp.7806-7811.

[20] S. Sakthivel, M.V. Shankar, M. Palanichamy, B. Arabindoo, V. Murugesan (2002), "Photocatalytic decomposition of leather dye - Comparative study of TiO_2 supported on alumina and glass beads", *J. Photochem. Photobiol. A*, **148**, pp.153-159.

[21] S. Ke, X. Cheng, Q. Wang, Y. Wang, Z. Pan (2014), "Preparation of a photocatalytic TiO_2/$ZnTiO_3$ coating on glazed ceramic tiles", *Ceram. Int.*, **40**, pp.8891-8895.

[22] S.N. Hosseini, S.M. Borghei, M. Vossoughi, N. Taghavinia (2007), "Immobilization of TiO_2 on perlite granules for photocatalytic degradation of phenol", *Appl. Catal. B*, **74**, pp.53-62.

[23] Y. Shavisi, S. Sharifnia, S.N. Hosseini, M.A. Khadivi (2014), "Application of TiO_2/perlite photocatalysis for degradation of ammonia in wastewater", *J. Ind. Eng. Chem.*, **20**, pp.278-283.

[24] D. Herskovitch, I.J. Lin (1996), "Upgrading of raw perlite by a dry magnetic technique", *Mag. Elect. Sep.*, **7**, pp.145-161.

[25] J. Rodriguez-Carvajal (2001), "Recent developments of the program FULLPROF. Commission of Powder Diffraction", *IUCr Newsletter*, **26**, pp.12-19.

[26] W.R. Taylor (1990), "Application of infrared spectroscopy to studies of silicate glass structure: Examples from the melilite glasses and the systems Na_2O-SiO_2 and Na_2O-Al_2O_3-SiO_2", *Proc. Indian Acad. Sci. (Earth Planet Sci.)*, **99**, pp.99-117.

[27] K.S. Babu, A.R. Reddy, C. Sujatha, K.V. Reddy, A.N. Mallika (2013), "Synthesis and optical characterization of porous ZnO", *J. Adv. Ceram.*, **2**, pp.260-265.

[28] A.C. Tas, P.J. Majewski, F. Aldinger (2002), "Synthesis of gallium oxide hydroxide crystals in aqueous solutions with or without urea and their calcination behavior", *J. Am. Ceram. Soc.*, **85**, pp.1421-1429.

[29] Y. Zhao, R.L. Frost, J. Yang, W.N. Martens (2008), "Size and morphology control of gallium oxide hydroxide GaO(OH), nano- to micro-sized particles by soft-chemistry route without surfactant", *J. Phys. Chem. C*, **112**, pp.3568-3579.

[30] H. Zhang, C. Hu (2011), "Effective solar absorption and radial microchannels of SnO_2 hierarchical structure for high photocatalytic activity", *Catal. Commun.*, **14**, pp.32-36.